Journal of Experimental and Theoretical Physics, Vol. 95, No. 2, 2002, pp. 181–193.
Translated from Zhurnal Éksperimental'noĭ i Teoreticheskoĭ Fiziki, Vol. 122, No. 2, 2002, pp. 211–226.

Solar Neutrino Flux Measurements by the Soviet–American Gallium Experiment (SAGE) for Half the 22-Year Solar Cycle

J. N. Abdurashitov[a], E. P. Veretenkin[a], V. M. Vermul[a], V. N. Gavrin[a, *], S. V. Girin[a], V. V. Gorbachev[a], P. P. Gurkina[a], G. T. Zatsepin[a], T. V. Ibragimova[a], A. V. Kalikhov[a], T. V. Knodel[a], I. N. Mirmov[a], N. G. Khairnasov[a], A. A. Shikhin[a], V. E. Yants[a], T. J. Bowles[b], W. A. Teasdale[b], J. S. Nico[c], J. F. Wilkerson[d], B. T. Cleveland[d], and S. R. Elliott[d]
SAGE Collaboration

[a]Institute for Nuclear Research, Russian Academy of Sciences, pr. Shestidesyatiletiya Oktyabrya 7a, Moscow, 117312 Russia
[b]Los Alamos National Laboratory, Los Alamos, New Mexico, 87545 USA
[c]National Institute of Standards and Technology, Gaithersburg, Maryland, 20899 USA
[d]University of Washington, Seattle, Washington, 98195 USA
**e-mail: gavrin@adonis.iasnet.ru*
Received February 15, 2002

Abstract—We present measurements of the solar neutrino capture rate on metallic gallium in the Soviet–American gallium experiment (SAGE) over a period of slightly more than half the 22-year solar cycle. A combined analysis of 92 runs over the twelve-year period from January 1990 until December 2001 yields a capture rate of $70.8^{+5.3}_{-5.2}$ (stat)$^{+3.7}_{-3.2}$ (sys) SNU for solar neutrinos with energies above 0.233 MeV. This value is slightly more than half the rate predicted by the standard solar model, 130 SNU. We present the results of new runs since April 1998 and analyze all runs combined by years, months, and bimonthly periods beginning in 1990. A simple analysis of the SAGE results together with the results of other solar neutrino experiments gives an estimate of $(4.6 \pm 1.2) \times 10^{10}$ neutrinos cm^{-2} s^{-1} for the flux of the electron *pp* neutrinos that reach the Earth without changing their flavor. The flux of the *pp* neutrinos produced in thermonuclear reactions in the Sun is estimated to be $(7.6 \pm 2.0) \times 10^{10}$ neutrinos cm^{-2} s^{-1}, in agreement with the value of $(5.95 \pm 0.06) \times 10^{10}$ neutrinos cm^{-2} s^{-1} predicted by the standard solar model. © *2002 MAIK "Nauka/Interperiodica"*.

1. INTRODUCTION

The last several years in neutrino astrophysics are characterized by outstanding achievements in solar neutrino studies. This is primarily because the large SuperKamiokande (SK) water Cherenkov detector [1] and the Sudbury neutrino observatory (SNO) [2] were put into operation. These telescopes record high-energy solar neutrinos from ^{8}B decay in real time and have high count rates.

The data obtained with these two giant new-generation neutrino telescopes make a crucially important complement to the available data from chlorine and gallium radiochemical experiments [3–5] and from the Kamiokande experiment [6]. Comparison of the SK data on elastic scattering of solar neutrinos by electrons with SNO data on charged currents indicates that, together with electron neutrinos, neutrinos of other flavors arrive at the Earth from the Sun. A combined analysis of the results from all these experiments provides compelling evidence that some of the electron neutrinos produced in thermonuclear reactions in the Sun change their flavor on their way to the Earth.

Investigating the details of the change in the flavor of solar neutrinos requires constructing neutrino telescopes of the next generation. These telescopes will record the low-energy part of the solar neutrino spectrum below 2 MeV, which contains the continuous spectra of *pp* neutrinos and neutrinos from the CNO cycle as well as monoenergetic lines from ^{7}Be and *pep* neutrinos.

Despite a number of promising ideas of detecting low-energy neutrinos in real time widely discussed today [7], only radiochemical gallium experiments are currently capable of observing and providing information on this part of the solar neutrino spectrum. The low threshold (233 keV) of the neutrino capture reaction ^{71}Ga(ν_e, e^-)^{71}Ge [8] allows the principal component of the solar neutrino spectrum, *pp* neutrinos, to be measured. If exotic hypotheses are excluded, the flux of these neutrinos is determined by energy release in the Sun and does not depend on solar-model parameters. These parameters significantly affect the rates of subsequent reactions in the chain of thermonuclear fusion in the Sun.

The expected neutrino capture rate on ^{71}Ga calculated using the standard solar model (SSM) is 128^{+9}_{-7} SNU[1] [9], with the contribution of *pp* neutrinos being

[1] SNU = 1 interaction per second in a target containing 10^{36} atoms of the isotope interacting with neutrinos.

dominant, 69.7 SNU. As follows from the same calculations, the contributions of neutrinos from ^{7}Be and ^{8}B decays are 34.2 and 12.1 SNU, respectively. The independently calculated value of 127.2 SNU [10] may suggest that the neutrino capture rate on gallium is insensitive to solar-model parameters.

From the SNO and SK measurements, we know the neutrino flux from ^{8}B decay with a high accuracy and what part of it is produced by the electron neutrinos which reach the Earth. In the immediate future, the KamLAND experiment [11] is expected to significantly reduce the range of possible oscillation parameters for electron neutrinos. This experiment and the BOREXINO experiment [12] will give the ^{7}Be neutrino flux with a high accuracy. By subtracting the ^{7}Be and ^{8}B components of the solar neutrino spectrum from the result of the gallium experiment, we will obtain a fundamental astrophysical parameter, the neutrino flux from the *pp* reaction (with a minor contribution of neutrinos from the *pep* reaction and the CNO cycle). The latter can be determined by comparing the SK results with those of the chlorine experiment. At the end of this paper, we give a preliminary estimate of the *pp*-neutrino flux by using the currently available experimental data. Since only a gallium experiment can provide for these measurements in the foreseeable future, it is crucially important that both gallium experiments, SAGE [4] and GNO [13] (the successor to GALLEX), continue their measurements so asto improve the accuracy of their results.

Previously [4], we described the SAGE experiment in detail, including germanium extraction from the gallium target, the counting of single ^{71}Ge atoms, and analysis of the data obtained. In [4], we presented the SAGE results for the period from January 1990 until December 1997. In this paper, we briefly describe basic principles of this experiment, perform a statistical analysis of the 1998–2001 data, and present the results of new analyses of some systematic uncertainties. In conclusion, we discuss the importance of the SAGE results for solar and neutrino physics.

2. AN OVERVIEW OF THE SAGE EXPERIMENT

2.1. The Laboratory of the Gallium–Germanium Neutrino Telescope

SAGE measurements are carried out at the gallium–germanium neutrino telescope (GGNT) placed in a specially constructed deep underground laboratory at the Baksan Neutrino Observatory (Institute for Nuclear Research, Russian Academy of Sciences) in the Northern Caucasus, at the foot of Mount Elbrus [14]. The underground complex of the GGNT laboratory is located in a horizontal tunnel that runs into the Andyrchi Mountain, at a distance of 3.5 km from the entrance. The main room of the laboratory is an experimental hall 60 m long, 10 m wide, and 12 m high. The rocks above the laboratory produce a shield from cosmic-ray muons that is equivalent to 4700-m-thick water and attenuate the muon flux by a factor of 10^7. The measured muon flux is $(3.03 \pm 0.10) \times 10^{-9}$ cm^{-2} s^{-1} [15]. To reduce the neutron and gamma-ray background from the surrounding rocks, the hall is clad with 600-mm-thick low-radioactivity concrete and with a 6-mm-thick steel sheet. The flux of neutrons with energy 1.0–11.0 MeV in the laboratory does not exceed 2.3×10^{-7} cm^{-2} s^{-1} [16]. There are also rooms for research on analytical chemistry, for a ^{71}Ge decay detection system, and for a low-background Ge semiconductor detector. Several rooms for auxiliary measurements are in the laboratory buildings located on the surface.

2.2. Procedures of the Experiment

The gallium target of the telescope currently contains about 50 t of gallium in the form of a liquid metal in seven chemical reactors. A measurement of the solar neutrino capture rate (run) begins with the addition to the gallium target of a stable germanium carrier in the form of a Ga–Ge alloy with a known germanium content, in the amount of 350 μg, which is uniformly distributed between all reactors. The reactor contents are well mixed to uniformly distribute germanium in the bulk of gallium.

On completion of the exposure (four weeks), the germanium carrier together with ^{71}Ge atoms from the solar neutrino capture reaction and from background reactions is extracted from the gallium by using the operations described in [4, 17]. The final stage of chemical extraction involves the synthesis of monogermane (GeH_4), which is placed in a proportional counter in a mixture with 70–90% of Xe. The total extraction efficiency, the ratio of the Ge mass in the monogermane to the initial mass of the Ge carrier, generally lies within the range of 80–90%. The systematic uncertainty in the extraction efficiency is 3.4%, mainly due to an uncertainty in the mass of the added and extracted carrier. About 0.1% of the gallium is dissolved during each extraction, passing into a muriatic solution in the form of chloride. The gallium-containing solutions are reprocessed to recover and purify gallium; subsequently, gallium must be returned to the target.

After its filling, the proportional counter is placed in the well of a NaI detector that is within a massive passive shield, where ^{71}Ge decays are counted for about five months. ^{71}Ge decays by electron capture with a half-life of 11.43 days. The low-energy Auger electrons from the *K* and *L* shells and the X-ray photons emitted when the electron shells are deexcited produce nearly point ionization in the counter gas. Therefore, the pulse from ^{71}Ge decay taken from the counter has a rapidly rising leading edge. In contrast, the ionization tracks from most of the background events have an appreciable length, and, accordingly, the fronts of the pulses from such events rise more slowly. Thus, we select event candidates for ^{71}Ge decay by the pulse energy in the proportional counter, which must correspond to the energy of the K or L peak, and by the rise time of the pulse front. In addition, an event should not have coincidences with the pulse from the NaI detector, because no γ-ray photons are emitted during ^{71}Ge decay.

The electronics for data acquisition was improved as the experiment developed. During the first two years, the amplitude-differentiated pulse (ADP) technique was used. This technique provided the selection of events in the K peak (10.4 keV) but could not be used to select events in the L peak (1.2 keV), which is more sensitive to instability of the electronics and in which the background is higher. In 1992, an eight-channel counting system was constructed. It consists of a 1-GHz digital oscilloscope that was used to record the pulse shape from the counters. The pulse amplitude and front rise time (T_N) can be determined by fitting the recorded pulse shape [18]. All results for the L peak and most of the results for the K peak were obtained from such an analysis of the pulse shape.

After their filling, the counters are regularly calibrated with a ^{55}Fe source (5.9 keV) through a window in the counter iron cathode. Additional calibrations with a ^{109}Cd source, whose emission produces the characteristic radiation of the iron cathode (6.4 keV) along the entire counter length, allow one to make a correction in the ^{71}Ge peak positions due to the buildups of polymers on the anode wire during prolonged operation of the counter. In addition, the characteristic radiation from a ^{109}Cd–Se source (1.4 and 11.2 keV) is used to check the energy scale within the measurement range for linearity.

The pulse energy can be determined by integrating the pulse shape for 800 ns after the pulse begins. The positions of the ^{71}Ge peaks corrected for counter polymerization and the widths of the energy windows corresponding to these peaks, which are taken to be twice the peak width at half maximum, are calculated from the ^{55}Fe calibration. Increasing the width of the energy windows causes no appreciable increase in the counting efficiency of ^{71}Ge decays but significantly degrades the signal-to-noise ratio.

If the peak position changes between two calibrations, then the window for energy selection is linearly shifted in time between the two calibrations. The change in amplification between calibrations typically does not exceed a few percent, which gives an uncertainty in the counting efficiency of no more than 3.1%.

In order to determine the rise times of the pulse fronts during ^{71}Ge decay, we carried out measurements in each counter channel using counters with ^{71}GeH$_4$ added to the gas mixture. The rise times T_N for all the events selected within the energy windows of the K and L peaks were arranged in increasing order. Subsequently an upper limit was set in such a way as to exclude 5% of events. The related small loss of counting efficiency is offset by a significant reduction in the number of background events. The derived ranges for T_N in the K and L peaks are, respectively, 0.0 to 18.4 ns and 0.0 to 10.0 ns. The variations attributable to gas filling of the counters and to differences of the various counter channels are 1.2 ns, which introduces an uncertainty in the efficiency of about ±1%.

Table 1 gives the parameters of the 35 runs from 1998–2001 that are used for the solar neutrino measurements.

3. STATISTICAL ANALYSIS OF THE SOLAR DATA

After the counting of ^{71}Ge decays in the proportional counter is finished, the selected (according to the criteria) ^{71}Ge events are called a data set. A maximum of the likelihood function [19] is sought for the events from each data set. In constructing this function, we assume that an event is caused by an unknown constant (in time) background and by ^{71}Ge decays whose number exponentially decreases with time. To minimize the possible effect of radon and its daughter elements that enter the passive shield during periodic counter calibrations and whose decays can imitate ^{71}Ge decays, we exclude from our analysis 2.6 h after each closure of the passive shield. The radon that is brought into the gas volume of the counter itself during its filling (several atoms) is very dangerous for measurements of the number of ^{71}Ge decays in the counters. Most of the radon decays within a counter produce slow pulses with energies above the energy range of the ^{71}Ge decay detection system (called overflow pulses), but about 8% of the decays of radon and its daughter elements produce fast pulses that are indistinguishable from ^{71}Ge pulses. The chain of radon decays leads to a long-lived isotope (^{210}Pb) after about 50 min, on average; excluding 15 min before each overflow pulse and 3 h after, we remove the overwhelming majority of events from the radon that decays within the counter.

The ^{71}Ge production rate is determined by the position of the maximum of the likelihood function for each data set. We calculate the statistical error by integrating this function over all possible background count rates. In the derived likelihood function, which now depends on the ^{71}Ge production rate alone, we find the minimum range of rate which contains 68% of the total area under the curve. This procedure is carried out separately for the events selected in the L and K peaks. The likelihood function for analysis of several runs (and for a combined analysis of the events selected in the L and K peaks in individual runs) is obtained by multiplying the likelihood functions for individual data sets with the additional requirement that the ^{71}Ge production rate per unit gallium mass be constant and that the background count rates be different for each data set. In our analysis, we take into account the small change in the ^{71}Ge

Table 1. The parameters of all runs since April 1998 used in our analysis to determine the solar neutrino flux

Exposure date	Mean exposure date	Exposure time, days	Ga mass, t	Extraction efficiency	Counter name	Pressure, mm Hg	% GeH_4	Working voltage, V	*K*-peak efficiency	*L*-peak efficiency	Polymerization coefficient
Apr. 98	1998.225	44.9	48.05	0.85	A13	695	37.0	1480	0.243	0.219	1.01
May 98	1998.347	30.0	51.17	0.91	LY4	690	29.5	1366	0.238	0.245	1.00
July 98	1998.477	45.6	51.06	0.90	A12	680	32.0	1414	0.235	0.237	1.00
Aug. 98	1998.611	45.7	50.93	0.89	LA51	660	27.0	1356	0.234	0.244	1.04
Oct. 98	1998.745	45.8	50.81	0.92	A13	680	32.0	1404	0.244	0.212	1.00
Nov. 98	1998.883	45.8	50.68	0.92	LY4	680	26.5	1322	0.238	0.244	1.00
Jan. 99	1999.014	44.7	50.54	0.92	A12	700	30.0	1398	0.239	0.241	1.00
Feb. 99	1999.130	38.7	50.43	0.89	LA51	705	11.0	1194	0.248	0.234	1.05
Apr. 99	1999.279	51.7	50.29	0.89	A13	665	13.5	1206	0.253	0.231	1.05
June 99	1999.417	46.7	50.17	0.87	LY4	670	11.0	1140	0.246	0.239	1.00
July 99	1999.551	45.7	50.06	0.90	L116	635	12.5	1164	0.243	0.244	1.03
Sept. 99	1999.685	45.7	49.91	0.91	LA51	660	11.5	1172	0.242	0.238	1.05
Oct. 99	1999.801	38.7	49.78	0.90	A13	665	12.5	1186	0.254	0.202	1.01
Jan. 00	2000.035	28.8	49.59	0.91	LA51	700	13.5	1224	0.324	0.310	1.05
Feb. 00	2000.127	30.7	49.48	0.83	LY4	646	10.4	1130	0.320	0.316	1.01
Mar. 00	2000.207	28.8	49.42	0.91	A13	665	14.5	1206	0.332	0.329	1.10
May 00	2000.359	30.7	49.24	0.92	LA116	705	14.0	1244	0.329	0.315	1.03
June 00	2000.451	33.7	49.18	0.84	LA51	652	12.0	1160	0.317	0.314	1.03
July 00	2000.541	32.0	49.12	0.92	LY5	670	13.8	1182	0.321	0.316	1.01
Aug. 00	2000.626	31.3	49.06	0.73	A13	707	9.5	1176	0.343	0.321	1.08
Sept. 00	2000.701	27.7	49.00	0.89	A12	690	14.7	1224	0.324	0.312	1.00
Oct. 00	2000.796	30.7	48.90	0.84	LA116	734	9.4	1188	0.337	0.303	1.03
Nov. 00	2000.876	28.7	48.84	0.93	LA51	680	11.9	1196	0.345	0.330	1.03
Dec. 00	2000.958	30.7	48.78	0.93	LY4	697	12.0	1174	0.327	0.312	1.02
Feb. 01	2001.122	29.8	41.11	0.87	LA116	287	9.2	1144	0.330	0.314	1.04
Mar. 01	2001.214	33.4	48.53	0.92	LA51	635	13.5	1180	0.314	0.317	1.02
Apr. 01	2001.290	22.7	48.43	0.90	YCT1	695	13.1	1210	0.344	0.333	1.00
May 01	2001.373	31.7	48.37	0.88	YCT2	625	14.9	1178	0.332	0.342	1.00
June 01	2001.469	31.7	48.27	0.92	YCT3	678	12.2	1190	0.342	0.334	1.00
July 01	2001.547	23.7	48.17	0.93	LA116	690	12.7	1196	0.328	0.315	1.03
Aug. 01	2001.624	28.7	48.11	0.59	A12	768	7.2	1148	0.340	0.302	1.00
Sept. 01	2001.701	27.7	48.06	0.90	YCT1	665	15.0	1204	0.338	0.337	1.00
Oct. 01	2001.793	30.7	47.96	0.88	YCT2	758	12.2	1210	0.354	0.326	1.00
Nov. 01	2001.887	34.8	47.91	0.92	YCT3	685	14.2	1210	0.342	0.335	1.00
Dec. 01	2001.955	22.8	47.86	0.86	YCT4	685	11.4	1176	0.344	0.333	1.00

Note: The *K*- and *L*-peak efficiencies are defined as the ratio of the number of ^{71}Ge decays recorded in the corresponding energy range to the total number of ^{71}Ge decays. The efficiencies include the efficiencies of energy selection (0.98) and selection by the pulse-front rise time (0.95); they take into account the fact that the data acquisition system in 1996–1999 contained an error in the trigger logic (0.76). The polymerization coefficient is the correction coefficient of the energy scale determined from the peak ratio in ^{55}Fe and ^{109}Cd calibrations.

production rate due to the orbital eccentricity of the Earth which leads to a 3% annual change in distance from the Sun. The position of the maximum of the combined likelihood function sets the global ^{71}Ge production rate. The 68% confidence interval is determined by the production rates at which the function decreases by a factor of 0.606 from its maximum value, all other variables being maximized. The results of our analysis

Table 2. Results of our analysis of the data from all runs since April 1998

Extraction time	Number of ^{71}Ge candidate events	Number of ^{71}Ge decays	Result, SNU	68% confidence interval, SNU	Nw^2	Probability, %
Apr. 98	39	5.4	75	26–134	0.052	72
May 98	23	3.4	44	10–88	0.051	68
July 98	22	4.8	61	24–108	0.065	52
Aug. 98	33	3.6	46	5–97	0.039	84
Oct. 98	40	3.8	45	4–95	0.028	95
Nov. 98	32	5.9	67	28–116	0.101	30
Jan. 99	21	4.5	56	15–107	0.036	84
Feb. 99	16	1.6	24	0–67	0.114	28
Apr. 99	10	1.8	38	5–83	0.105	36
June 99	14	12.9	172	123–232	0.048	80
July 99	17	5.5	103	49–172	0.118	20
Sept. 99	20	7.1	93	43–154	0.099	28
Oct. 99	16	10.0	138	80–206	0.066	56
Jan. 00	24	5.4	63	23–111	0.060	59
Feb. 00	21	9.1	107	63–157	0.058	55
Mar. 00	19	10.1	117	78–165	0.046	79
May 00	15	0.0	0	0–32	0.143	40
June 00	17	1.4	23	0–75	0.179	17
July 00	29	6.4	69	33–111	0.088	34
Aug. 00	14	5.2	74	39–117	0.086	33
Sept. 00	30	9.2	111	64–166	0.093	24
Oct. 00	14	3.0	37	8–75	0.020	99
Nov. 00	25	2.9	32	0–73	0.208	9
Dec. 00	27	7.6	81	43–127	0.062	68
Feb. 01	21	6.3	79	43–125	0.088	34
Mar. 01	18	3.8	44	14–80	0.120	24
Apr. 01	17	6.7	76	43–117	0.074	45
May 01	21	11.9	127	90–171	0.088	31
June 01	20	9.4	93	57–135	0.025	96
July 01	9	2.1	24	0–58	0.033	92
Aug. 01	21	5.4	90	38–155	0.065	57
Sept. 01	10	2.1	22	0–53	0.139	18
Oct. 01	12	7.5	73	44–109	0.082	41
Nov. 01	15	2.6	23	0–54	0.084	38
Dec. 01	9	5.2	62	34–101	0.063	70
Combined result	711	191.8	67	60–74	0.080	42

Note: The test statistics of Nw^2 is described and interpreted in [20]. The probability that the sequence of measured events arose from the combination of ^{71}Ge decay plus background events at a constant count rate was calculated by the Monte Carlo method and is given in the last column. The accuracy of the quoted probabilities is approximately 1.5% for individual runs and about 4% for the combined result.

of recent extractions are given in Table 2. The results of all SAGE runs are shown in Fig. 1.

After the publication of our paper [4], which contains the measurements made from January 1990 until December 1997, we found that we used an erroneous data acquisition program from June 1996 until December 1999. At the beginning of this period, a failed electronics module in the data acquisition system was replaced, which required modifying the system for

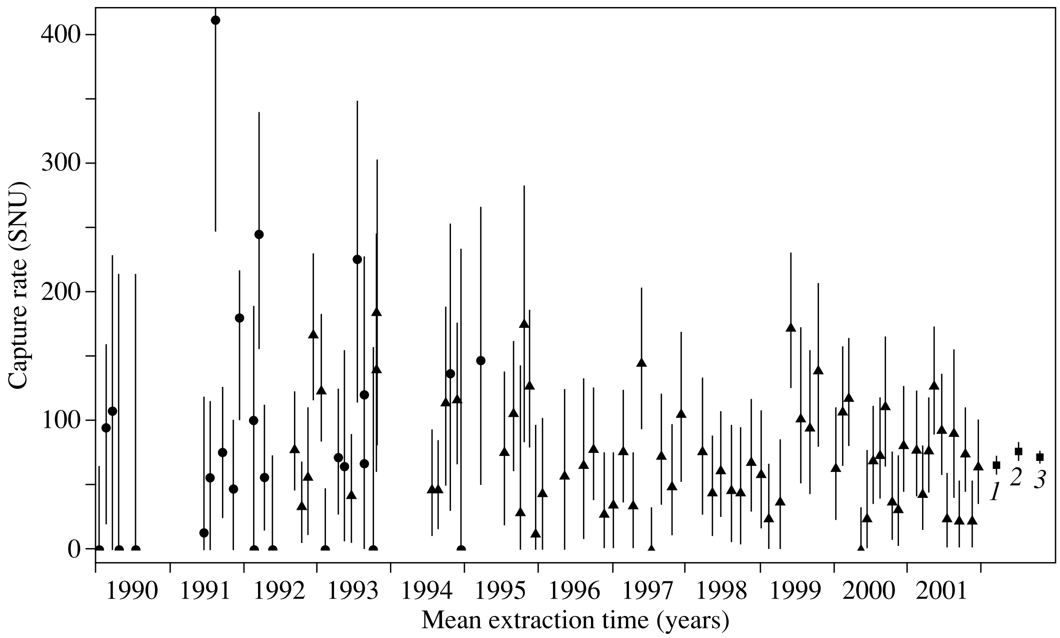

Fig. 1. The capture rate from all SAGE extractions versus time: the triangles are for the *L* and *K* peaks and the circles are for the *K* peak alone; the vertical bars near each point correspond to a statistical error of 68%. (*1*) The results of analysis for the *L* peak, (*2*) the results of analysis for the *K* peak, and (*3*) the combined result for the entire data set.

determining the coincidences of the pulses from events in the NaI detector and events in the proportional counters. The new system entailed a change in the data acquisition program and an error in the trigger logic was introduced. Because of this error, 23.9 ± 0.4 (stat) ± 0.5 (sys)% of triggers were lost. This error artificially underestimated the results of individual runs which were counting during this period, and affected the combined result. The corrected results are given in [21].

Table 3. Systematic effects and the related uncertainties in the measured neutrino capture rate (SNU). The extraction and counting efficiencies are based on a capture rate of 70.8 SNU

Extraction efficiency	Ge-carrier mass	±1.5
	Extracted Ge mass	±1.8
	Ge-carrier residue in reactor	±0.6
	Gallium mass	±0.2
Counting efficiency	Volume efficiency	±1.3
	Gain shifts	+2.3
	Resolution	–0.4, +0.5
	Rise time limits	±0.7
	Exposure time and time before counting begins	±0.6
Backgrounds	Neutrons	< –0.02
	U and Th	< –0.7
	Cosmic-ray muons	< –0.7
	Internal radon	< –0.2
	External radon	0
	Other Ge isotopes	< –0.7
Total		–3.2, +3.7

4. SYSTEMATIC EFFECTS

Table 3 presents the systematic effects that can affect the measured capture rate of solar neutrinos. These effects can be arbitrarily broken down into three main categories: uncertainties related to the extraction efficiency, the counting efficiency of ^{71}Ge decays, and backgrounds. Some of these effects were considered above, and the remaining ones are briefly discussed in this section. The counter efficiency was determined in a series of measurements with different gas fillings; these fillings contained ^{71}Ge, ^{37}Ar, and ^{69}Ge. The uncertainties in the measured counter efficiency are attributable to uncertainties in the volume efficiency, edge effects, and gas-mixture composition. A quadratic summation of these effects yields an uncertainty of ±1.8% in the counter efficiency.

The uncertainties also result from the systematic effects attributable to the background production sources of germanium isotopes in the gallium target and radon decays inside and near the counters. Limits on the ^{71}Ge production rate by the (*n*, *p*) reaction on ^{71}Ga were obtained from the measured fluxes of fast neutrons [16, 22] and cosmic-ray muons in the underground laboratory [15]. The limiting concentrations of U and Th in gallium, which can also give rise to germanium isotopes, were measured with a germanium semiconductor detector [23] and a mass spectrometer [24]. The total ^{71}Ge production rate from all these processes does not exceed 1 SNU.

Radon is removed from the internal volume of the passive shield where the counters are located by evaporating liquid nitrogen. Special antiradon gas mixture purification procedures are used during the filling to reduce the possibility of radon penetration into the counter. The effect of the remaining radon on the measured ^{71}Ge production rate was studied through special measurements with counters with the addition of some amount of radon to their gas mixture and when investigating the counter response to external γ-ray radiation [25, 26]. The upper limits on the systematic error due to radon decays inside and outside the counter obtained from these studies are 0.2 and 0.03 SNU, respectively.

The decays of ^{68}Ge and ^{69}Ge produced in the gallium target in background processes can imitate ^{71}Ge events. The amount of ^{68}Ge produced in cosmic-ray muon interactions can be estimated from the expected ^{71}Ge production rate in muon interactions. It was found to be 0.012 ± 0.006 atom per day in 60 t of gallium [4, 27]. For the measured ratio of the ^{68}Ge and ^{71}Ge production cross sections in the reactions with gallium of muons with energy of 280 GeV equal to 2.1 ± 0.05 [28] in 50 t of gallium per day, 0.022 ± 0.013 ^{68}Ge atoms are produced. For the ^{68}Ge half-life of 271 days, these pulses are distributed almost uniformly in time during the counting, increasing only the mean background count rate. However, during the initial counting period, these pulses can cause an increase in the ^{71}Ge count rate. Monte Carlo calculations show that for typical parameters of our measurements—an exposure time of 30 days, a gallium mass of 50 t, an extraction efficiency of 0.9, a counting efficiency (L peak + K peak) of 0.6, and a background count rate (L peak + K peak) of 0.175 event per day—a ^{68}Ge production rate of 0.022 event per day gives a contribution of 0.0085 event per day to the ^{71}Ge production rate, which is equivalent to 0.05 SNU.

The ^{69}Ge isotope is produced in the gallium target through the interaction of α particles from internal radioactivity of the target and the neutrons emitted by the surrounding rocks and in the interactions of solar neutrinos with cosmic-ray muons. The ^{69}Ge production rate in 60 t of gallium is 0.21 atoms per day [4] with an uncertainty of about 50%. Since most of the ^{69}Ge decays are accompanied by γ-ray radiation recorded by the NaI detector with 90% efficiency and since the counter begins to count about 1.5 days after extraction, only 0.045 events from ^{69}Ge are observed in one run; this is a factor of 100 fewer than the mean number of recorded ^{71}Ge decays. Thus, the background effect from ^{69}Ge is no more than 0.7 SNU.

The capabilities of the ^{71}Ge decay detection system and the large number of measurements allowed us to search for events related to ^{68}Ge and ^{69}Ge decays in the solar runs [29]. The event selection techniques and efficiency were determined with allowance made for peculiarities of the decays of these isotopes. The inferred ^{68}Ge production rate is $0.18^{+0.13}_{-0.12}$ atom in 60 t of gallium per day, which is approximately a factor of 7 higher than the expected value, although these values are in agreement within the error limits. Since the ^{68}Ge production rate was derived from muon experiments with smaller errors, we use this value to determine the uncertainty. The possibility of directly measuring the production rate of germanium isotopes in cosmic-ray muon interactions for the underground conditions of the Baksan Neutrino Observatory (Institute for Nuclear Research, Russian Academy of Sciences) was explored in [29].

A similar search for ^{69}Ge events shows that the ^{69}Ge production rate in 60 t of gallium does not exceed 0.49 atom per day. This is in good agreement with the above value. The inferred constraint does not rule out the possibility that the production rate of this isotope during cosmic-ray muon interactions can be higher than its predicted value, which may be indicated by analysis of ^{68}Ge events.

5. RESULTS

In this section, we present the measurements of the solar neutrino capture rate in gallium performed from January 1990 until December 2001. The capture rate determined by analyzing 92 runs and 158 individual data sets is $70.8^{+5.3}_{-5.2}$ SNU. Here, only the statistical uncertainties are given. We selected 1723 events within the designated boundaries of the L and K peaks of ^{71}Ge, 406.4 of which were attributed to ^{71}Ge by a time analysis (the total live counting time is 29.5 yr). The results of our analysis of the events selected separately in the L and K peaks are $64.8^{+8.5}_{-8.2}$ and $74.4^{+6.8}_{-6.6}$ SNU, respectively. Agreement between these two results serves as a check on the quality of the event selection criteria. The total systematic uncertainty is obtained by a quadratic summation of all the systematic contributions presented in Table 3. Thus, the SAGE result is $70.8^{+5.3\,+3.7}_{-5.2\,-3.2}$ SNU. For comparison, the latest GNO result (including GALLEX data) is $74.1^{+5.4\,+4.0}_{-5.4\,-4.2}$ SNU [13]. With the quadratic summation of statistical and systematic uncertainties, the SAGE result is $70.8^{+6.5}_{-6.1}$ SNU.

5.1. Checking the ^{71}Ge Extraction Efficiency

The technologies used in the experiment allow a few ^{71}Ge atoms produced by neutrino interactions to be chemically extracted from the target containing 5×10^{29} gallium atoms with a high, well-known efficiency. To measure this efficiency, about 350 μg of a stable germanium carrier is added to the gallium at the beginning of each exposure. In this case, given the carrier, there are 10^{11} gallium atoms per one germanium atom. We carried out a number of auxiliary measurements, which

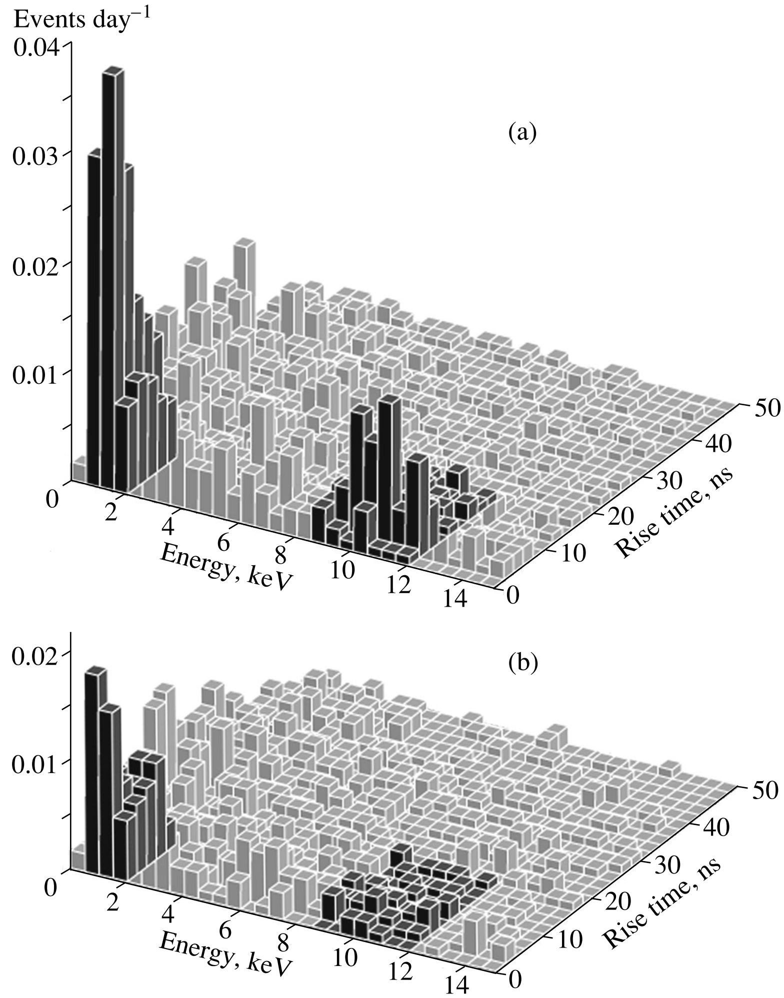

Fig. 2. The distribution of events in energy and in pulse rise time for all the runs in which these quantities were determined from the pulse shape. (a) The events recorded within the first 22.86 days of counting after extraction for all runs (except the May 1996 extraction). The total live counting time is 1169.9 days. The positions of the *L* and *K* peaks of ^{71}Ge determined from calibrations are indicated in dark gray. (b) The same histogram for all the events that were recorded during an equal live time interval beginning 100 days after extraction.

confirmed the efficiency of our technology for extracting single ^{71}Ge atoms from metallic gallium.

A germanium carrier with a known amount of ^{71}Ge included in its composition was added to the reactor containing 7 t of gallium. We made three extractions and measured the number of atoms of extracted ^{71}Ge in each of them. Our results [17] showed that the extraction efficiencies of a stable germanium carrier and ^{71}Ge are the same.

The objective of the second experiment was to determine whether ^{71}Ge, whose atoms can be produced in the reverse β-decay reaction in an excited or ionized state, forms chemical bonds that prevent its efficient extraction. We prepared and carried out several measurements to directly test this possibility, in which the β decay of radioactive gallium isotopes was observed in liquid metallic gallium. Our result [17] matches the expected value with 10% accuracy.

We checked the entire experiment (i.e., completely checked all experimental procedures, including the efficiency of chemical extraction, the counter efficiency, and the techniques of analysis) by using an artificial source of ^{51}Cr neutrinos with an intensity of 19.1 PBq (517 kCi) [30, 31]. The result, expressed as the ratio of the measured ^{71}Ge production rate to the expected rate, was (0.95 ± 0.12). This is evidence that the experimental efficiencies we use are correct and justifies the fundamental assumption of radiochemical experiments that the extraction efficiency of atoms produced in neutrino interactions does not differ from the carrier extraction efficiency.

5.2. Checking the Results of Analysis

Figure 2 provides clear evidence that we actually observe ^{71}Ge decay. This figure shows all events that survive the time cuts and that had no coincidences with pulses from the NaI detector. The expected positions of the L and K peaks of ^{71}Ge are highlighted in dark gray. These peaks are clearly present in the upper histogram, but they are absent in the lower panel, because ^{71}Ge has decayed by that time. Outside the peak regions, the numbers of events in Figs. 2a and 2b are approximately equal, because these events mostly have a background origin.

5.2.1. The time sequence of events. A major hypothesis of our analysis is that the time sequence of observed events for each run is a superposition of events from the decay of a fixed number of ^{71}Ge atoms and background events that occur at a constant rate. The quantity Nw^2 [20] and the corresponding fitting probability gives a quantitative measure of how well the counting data fit this hypothesis. These quantities, which were calculated for each data set, are presented in Table 2. There are runs with a low fitting probability, but the number of such runs is no more than that expected for normal statistical variations.

The Nw^2 method can also be used to estimate the fitting quality of the combined time sequences for all events of the L and K peaks for any combination of runs. The test statistics for the combined data set from all runs is $Nw^2 = 0.053$; the corresponding fitting probability is (72 ± 4.5)%. The fitting quality is seen from Fig. 3, in which the mean count rate of events in the L and K peaks from all runs is plotted against the time elapsed after extraction. An additional quantitative confirmation that ^{71}Ge is counted in the experiment can be obtained if the decay constant is allowed in the likelihood function to be a free parameter, as are the ^{71}Ge production rate and all background count rates. The half-life determined in this way for all the selected events in the L and K peaks is $9.7^{+1.5}_{-1.3}$ days, in agreement with the measured value of 11.43 days [32].

5.2.2. The ^{71}Ge production rate. Another hypothesis of our analysis is that the ^{71}Ge production rate is constant with time. As we see from Fig. 1, there are no appreciable deviations of the rate from its mean value within large statistical uncertainties.

The constancy of the production rate can also be considered by using the distribution function of the production rate, $C(p)$, defined as the fractional number of data sets in which the production rate is less than p. Figure 4 shows this distribution for all experimental data sets. Also shown here for comparison is the distribution obtained by the Monte Carlo method by assuming that the true production rate is 70.8 SNU. The two curves are close to each other, and they can be compared by calculating the test statistics Nw^2 [20]. This calculation yields $Nw^2 = 0.337$, which corresponds to a probability of 11%.

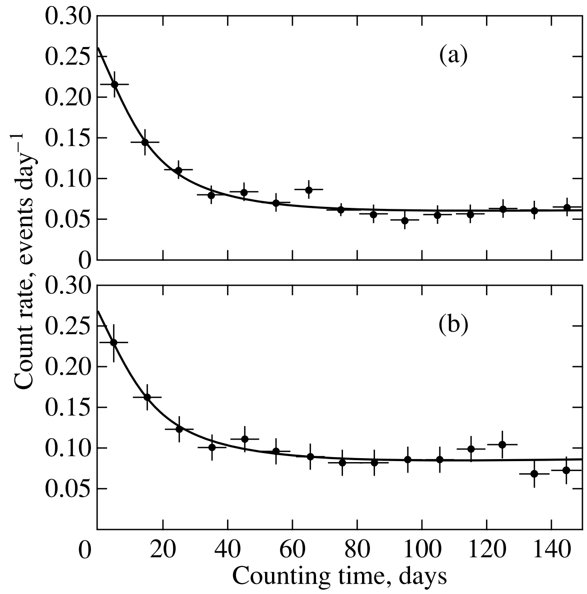

Fig. 3. The mean count rate of the events selected in the (a) K and (b) L peaks in all the runs since January 1990. The solid line represents the curve of ^{71}Ge decay with a half-life of 11.4 days plus a constant background count rate of events. The errors indicated by vertical bars near each point are proportional to the square root of the number of events. The horizontal bars represent the ±5-day time intervals within which the mean count rate of events is taken.

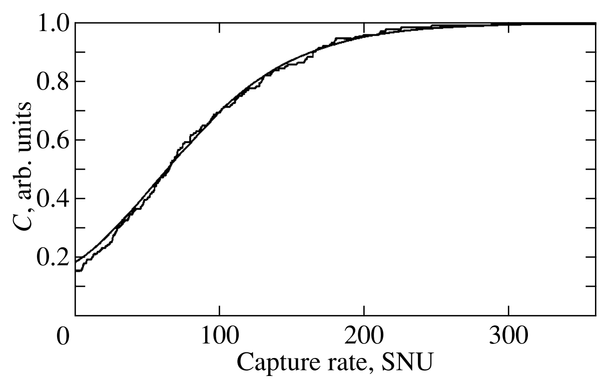

Fig. 4. Cumulative distribution functions for the neutrino capture rate measured in 158 SAGE data sets (histogram) and calculated by the Monte Carlo method (solid line). The capture rate in Monte Carlo calculations was taken to be 70.8 SNU.

5.3. Combining Data by Time

If vacuum oscillations are responsible for the low measured capture rate of neutrinos by gallium compared to that predicted by the SSM, then one might expect seasonal variations in the capture rate [33, 34]. Other phenomena can also lead to temporal variations (see, e.g., [35, 36]). Table 4 presents the results of our analysis of the SAGE runs combined in different ways—by months, by pairs of months, and by years. In none of these combinations is there irrefutable evidence of temporal variations. The results of our analysis of the runs combined by years are shown in Fig. 5. We see

Table 4. Results of our analysis of the data from SAGE runs combined by years, by months, and by pairs of months

Exposure period	Number of data sets	Number of ^{71}Ge-candidate events	Number fit to ^{71}Ge	Result, SNU	68% confidence interval, SNU	Nw^2	Probability, %
1990	5	43	4.9	43	2–78	0.260	9
1991	6	59	25.5	112	82–145	0.120	17
1992	13	145	39.8	76	59–95	0.047	68
1993	15	97	33.2	84	62–105	0.199	6
1994	10	155	24.1	73	51–98	0.027	95
1995	13	210	37.7	102	77–129	0.041	82
1996	10	121	19.4	56	34–79	0.064	51
1997	16	183	35.7	62	48–78	0.057	62
1998	12	189	26.7	56	39–75	0.064	60
1999	14	114	40.8	87	66–110	0.068	33
2000	22	235	62.2	67	55–80	0.102	29
2001	22	173	64.4	65	55–76	0.050	70
Jan.	11	129	24.8	58	37–80	0.082	35
Feb.	12	101	25.5	60	44–77	0.045	74
Mar.	9	129	34.5	102	79–127	0.043	78
Apr.	9	80	16.9	54	37–73	0.072	39
May	12	114	34.7	75	59–94	0.051	62
June	11	101	33.6	79	58–102	0.175	5
July	15	176	26.6	52	37–69	0.091	35
Aug.	15	161	38.7	78	60–96	0.058	51
Sept.	20	220	48.5	68	54–84	0.035	91
Oct.	17	169	40.3	73	56–91	0.080	45
Nov.	15	197	37.6	59	44–75	0.033	90
Dec.	12	147	46.4	105	84–127	0.040	89
Jan. + Feb.	23	230	50.5	59	46–73	0.095	34
Mar. + Apr.	18	209	49.2	75	61–91	0.026	>99
May + June	23	215	68.0	77	63–91	0.111	10
July + Aug.	30	337	65.4	65	53–78	0.075	50
Sept. + Oct.	37	389	88.7	71	60–82	0.041	85
Nov. + Dec.	27	344	84.3	78	66–91	0.040	85
Feb. + Mar.	21	230	58.8	77	63–91	0.037	84
Apr. + May	21	194	50.8	66	54–79	0.049	60
June + July	26	277	58.7	63	50–77	0.081	42
Aug. + Sept.	35	381	87.2	73	61–84	0.043	84
Oct. + Nov.	32	366	78.1	66	54–78	0.044	82
Dec. + Jan.	23	276	73.6	84	70–99	0.059	65
Feb. + Nov.	27	298	63.1	59	48–71	0.017	99
Mar. + Oct.	26	298	75.1	84	71–99	0.062	66
Apr. + Sept.	29	300	64.3	63	52–75	0.042	86
May + Aug.	27	275	73.3	77	64–89	0.045	75

Note: The runs are assigned to each time interval in accordance with the mean exposure time. The accuracy of estimating the probability is approximately 4%.

from this figure that the neutrino capture rate was constant during the entire data acquisition period. The test statistics under the assumption of a constant capture rate, 70.8 SNU, is $\chi^2 = 6.6$; for 11 degrees of freedom, this corresponds to a 83% probability.

6. THE *pp*-NEUTRINO FLUX

One of the prime objectives of the gallium experiment is to obtain the information required to determine the *pp*-neutrino flux that arrives at the Earth. In this section, we assess the state of this problem by using the currently available results of all solar neutrino experiments.

As follows from the SAGE, GALLEX, and GNO experiments, the mean capture rate of neutrinos in the gallium experiment is 72 ± 5 SNU. This rate is the sum of the rates from all components of the solar neutrino flux, which we designate as $[pp + {}^7\mathrm{Be} + \mathrm{CNO} + pep + {}^8\mathrm{B}|\mathrm{Ga}]_{\mathrm{exp}}$, where the subscript "exp" indicates that this is an experimentally measured quantity. Here, we ignore the *hep* neutrinos, because the contribution of this component is negligible, 0.05% of the total capture rate predicted by the SSM [9]. The only known component of the solar electron neutrino flux is ^{8}B neutrinos, whose flux was measured by SNO: $[{}^8\mathrm{B}|\mathrm{CNO}]_{\mathrm{exp}} = (1.75 \pm 0.15) \times 10^6$ electron neutrinos cm^{-2} s^{-1} [2]. The measured SNO and SK spectra are similar in shape to the spectrum predicted by the SSM. The measured SNO flux of electron neutrinos and the capture cross section for ^{8}B neutrinos from the SSM ($2.40^{+0.77}_{-0.36} \times 10^{-42}$ cm^2) can be used to determine the contribution of neutrinos from ^{8}B to the capture rate measured in gallium experiments, because the cross section for neutrino capture by gallium increases sharply with energy. This yields

$$[{}^8\mathrm{B}|\mathrm{Ga}]_{\mathrm{exp}} = 4.2^{+1.4}_{-0.7}\ \mathrm{SNU}.$$

Subtracting this value from the total capture rate measured in gallium yields the contribution in a gallium experiment from *pp* neutrinos and intermediate-energy neutrinos

$$[pp + {}^7\mathrm{Be} + \mathrm{CNO} + pep|\mathrm{Ga}]_{\mathrm{exp}} = 67.8^{+5.1}_{-5.2}\ \mathrm{SNU}.$$

The measured neutrino capture rate in a chlorine experiment is

$$[{}^7\mathrm{Be} + {}^8\mathrm{B} + \mathrm{CNO} + pep|\mathrm{Cl}]_{\mathrm{exp}} = 2.56 \pm 0.23\ \mathrm{SNU}$$

[3]. We again ignored the contribution of *hep* neutrinos, because it accounts for a mere 0.5% of the total capture rate predicted by the SSM. Since neutrinos with energies above 5 MeV give a dominant contribution in a chlorine experiment, we can again use the measured SNO flux and the cross section calculated for the SSM,

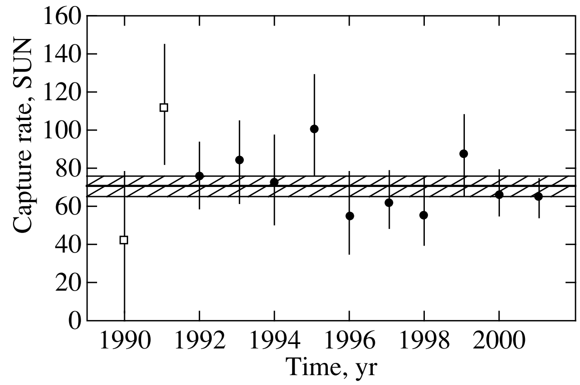

Fig. 5. Results of the measurements combined by years; open and filled symbols refer to K and $K + L$ peaks, respectively; the hatched region corresponds to the SAGE result of $70.8^{+5.3}_{-5.2}$ SNU. The data shown have a statistical error of 68%.

$(1.14 \pm 0.04) \times 10^{-42}$ cm^2. Thus, the contribution of ^{8}B neutrinos is

$$[{}^8\mathrm{B}|\mathrm{Cl}]_{\mathrm{exp}} = 2.0 \pm 0.2\ \mathrm{SNU}.$$

Subtracting this component yields the contribution of intermediate-energy neutrinos to the chlorine experiment

$$[{}^7\mathrm{Be} + \mathrm{CNO} + pep|\mathrm{Cl}]_{\mathrm{exp}} = 0.56 \pm 0.29\ \mathrm{SNU}.$$

The effect of neutrino oscillations is generally taken into account by introducing the so-called survival factor, the probability that neutrinos will preserve their flavor on their way to the Earth. For intermediate-energy neutrinos in the chlorine experiment, this factor can be determined from the ratio of the measured capture rate to that predicted by the SSM,

$$[{}^7\mathrm{Be} + \mathrm{CNO} + pep|\mathrm{Cl}]_{\mathrm{SSM}} = 1.79 \pm 0.23\ \mathrm{SNU}.$$

If we assume that the survival factor in the range of intermediate energies changes only slightly, then we may set it equal to

$$\frac{[{}^7\mathrm{Be} + \mathrm{CNO} + pep|\mathrm{Cl}]_{\mathrm{exp}}}{[{}^7\mathrm{Be} + \mathrm{CNO} + pep|\mathrm{Cl}]_{\mathrm{SSM}}} = 0.31 \pm 0.17.$$

Since neutrinos from ^{7}Be in the range of intermediate energies mainly contribute to the result of the chlorine experiment and since their spectrum is a monoenergetic line, the error in this factor can be estimated by assuming that the relative contribution of the remaining components to the error is the same as their predicted contribution to the SSM, i.e., 36%. Thus, we increase the uncertainty in the survival factor: $0.17 + 0.31 \times 0.36 = 0.28$.

The relative contributions of intermediate-energy neutrinos in Ga to the capture rate are approximately the same as those in Cl (e.g., from ^{7}Be neutrinos, 75% in Ga and 64% in Cl). This gives grounds to apply the survival factor determined for Cl to a gallium experiment, i.e.,

$$[^7\text{Be} + \text{CNO} + pep|\text{Ga}]_{\text{exp}}$$
$$= (0.13 \pm 0.28)[^7\text{Be} + \text{CNO} + pep|\text{Ga}]_{\text{SSM}}$$
$$= 14.4 \pm 13.0 \text{ SNU}.$$

Subtracting this contribution of intermediate-energy neutrinos from the capture rate in gallium obtained above yields the measured *pp*-neutrino capture rate in a gallium experiment,

$$[pp|\text{Ga}]_{\text{exp}} = [pp + {}^7\text{Be} + \text{CNO} + pep|\text{Ga}]_{\text{exp}}$$
$$- [^7\text{Be} + \text{CNO} + pep|\text{Ga}]_{\text{exp}} = 53.4 \pm 14.0 \text{ SNU}.$$

Since the capture cross section for *pp* neutrinos interacting with Ga in the narrow energy range, 0.23–0.42 MeV, does not change appreciably, we divide the measured capture rate by the calculated electron-neutrino capture cross section $(11.7 \pm 0.3) \times 10^{-46}$ cm^2 for the SSM and obtain the measured *pp*-neutrino flux on Earth: $(4.6 \pm 1.2) \times 10^{10}$ electron neutrinos cm^{-2} s^{-1}.

On the other hand, knowing the capture cross section and the survival factor, we can determine the *pp*-neutrino flux emitted in thermonuclear reactions in the Sun from the derived capture rate of neutrinos on gallium. If the neutrino oscillation parameters lie within the LMA range (the range of large mixing angles), which is now considered to be the preferred one, then the survival factor is 60% and the flux of the emitted *pp* neutrinos is $(7.6 \pm 2.0) \times 10^{10}$ cm^{-2} s^{-1}. This is in agreement with the value predicted by the SSM, $(5.95 \pm 0.06) \times 10^{10}$ neutrinos cm^{-2} s^{-1} [37, 38]. A significant part of the measurement error in the *pp*-neutrino flux stems from the fact that the energy dependence of the survival factor is not well known.

In calculating these *pp*-neutrino fluxes, we made several assumptions; the errors that arise in this case cannot be determined in a simple way. Therefore, the errors given here may have been underestimated. As was pointed out in the Introduction, we will be able to significantly reduce this error when the range of possible mass and mixing angle parameters will be limited by the KamLAND experiment and when the flux of ^{7}Be neutrinos will be directly measured, as expected in the BOREXINO experiment. In that case, the dominant error will be uncertainty in the measurements of the gallium experiment itself. Therefore, our efforts are now directed to reducing the statistical and systematic uncertainties in the SAGE experiment.

7. CONCLUSION

We have described the basic principles and techniques of the SAGE experiment and analyzed 92 extractions made over the twelve-year period from January 1990 until December 2001. The measured capture rate of solar neutrinos by gallium is $70.8^{+5.3}_{-5.2}$ SNU. Here, only the statistical uncertainties are given. Analysis of the well-known systematic effects showed that the total systematic uncertainty is smaller than the statistical error, being $^{+3.7}_{-3.2}$ SNU. Finally, we have examined the counting data and shown that there is good evidence that ^{71}Ge is being counted, that the counting data fit the hypotheses of our analysis, and that the counting data are self-consistent.

The SAGE result of 70.8 SNU accounts for 55% of the value predicted by the SSM [9, 10]. A check of systematic effects and our additional measurements, in particular, the experiment with a ^{51}Cr neutrino source [30, 31], suggest that the difference between our solar neutrino capture rate and the value predicted by the SSM (6.0σ, where σ is the standard deviation) is strong evidence that the flux of solar neutrinos with energies below 2 MeV is much lower than the expected flux. This was also shown for the ^{8}B-neutrino flux by the chlorine neutrino experiment and in the Kamiokande and CHO experiments. The SAGE result is even smaller than the minimum astrophysical capture rate of $79.5^{+2.3}_{-2.0}$ SNU [39].

The combined result of all solar neutrino experiments is discussed in several phenomenological papers [40–42]. Their main conclusion reduces to the following: the electron neutrinos produced in the Sun reach the Earth in a different flavor state, and Mikheev–Smirnov–Wolfenstein oscillations with the oscillation parameters in the LMA range are best suited as the mechanism of change in the flavor of solar neutrinos. A more accurate determination of the oscillation parameters requires additional data, particularly those obtained in experiments sensitive to low-energy neutrinos. To this end, the SAGE collaboration regularly performs solar neutrino extractions, every four weeks, from about 50 t of gallium, reducing the statistical error, and explores further possibilities for reducing the systematic uncertainties.

ACKNOWLEDGMENTS

We thank J.N. Bahcall, M. Baldo-Ceolin, G.T. Garvey, W. Haxton, V.A. Kuzmin, V.V. Kuzminov, V.A. Matveev, L.B. Okun, R.G.H. Robertson, V.A. Rubakov, A.Yu. Smirnov, A.N. Tavkhelidze, and many members of GALLEX and GNO for their continued interest and for stimulating discussions. We greatly appreciate the work of our prior collaborators O.L. Anosov, O.V. Bychuk, M.L. Cherry, R. Davis, Jr., I.I. Knyshenko, V.N. Kornoukhov, R.T. Kouzes, K. Lande, A.V. Ostrinsky, D.L. Wark, P.W. Wildenhain, and Yu.I. Zakharov.

This study was supported by the Russian Foundation for Basic Research (project nos. 96-02-18399, 99-02-16110b, and 00-15-96632), the Division of Nuclear Physics of the US Department of Energy (grant DEFG03-97ER4120), the International Science Foundation (grants M7F000 and M7F300), and the American Foundation for Civil Research and Development (grants RP2-159 and RP2-2253).

REFERENCES

1. S. Fukuda, Y. Fukuda, M. Ishitsuka, *et al.*, hep-ex/0103032; Phys. Rev. Lett. **86**, 5651 (2001); hep-ex/0103033; Phys. Rev. Lett. **86**, 5656 (2001).
2. Q. R. Ahmad, R. C. Allen, T. C. Andersen, *et al.*, nucl-ex/0106015; Phys. Rev. Lett. **87**, 071301 (2001).
3. B. T. Cleveland, T. J. Daily, R. Davis, Jr., *et al.*, Astrophys. J. **496**, 505 (1998).
4. J. N. Abdurashitov, V. N. Gavrin, S. V. Girin, *et al.*, astro-ph/9907113; Phys. Rev. C **60**, 055801 (1999).
5. W. Hampel, J. Handt, G. Heusser, *et al.*, Phys. Lett. B **447**, 127 (1999).
6. Y. Fukuda, T. Hayakawa, K. Inoue, *et al.*, Phys. Rev. Lett. **77**, 1683 (1996).
7. www.sns.ias.edu/~jnb/Meetings/lownu/index.html; www.sk.icrr.u-tokyo.ac.jp/lownu/index.html.
8. V. A. Kuz'min, Zh. Éksp. Teor. Fiz. **49**, 1532 (1965) [Sov. Phys. JETP **22**, 1051 (1966)].
9. J. N. Bahcall, M. C. Gonzalez-Garcia, and C. Peña-Garay, hep-ph/0111150.
10. A. S. Brun, S. Turck-Chieze, and P. Morel, astro-ph/9806272; Astrophys. J. **506**, 913 (1998).
11. A. Piepke, Nucl. Phys. B (Proc. Suppl.) **91**, 99 (2001).
12. G. Alimonti, C. Arpesella, H. Back, *et al.*, hep-ex/0012030; Astropart. Phys. **16**, 205 (2002).
13. M. Altmann, M. Balata, P. Belli, *et al.*, hep-ex/0006034; Phys. Lett. B **490**, 16 (2000).
14. V. N. Gavrin, V. N. Kornoukhov, and G. T. Zatsepin, Preprint IYaI AN SSSR P-0690 (1991).
15. V. N. Gavrin, V. É. Gurentsov, V. N. Kornoukhov, *et al.*, Preprint IYaI AN SSSR P-0698 (1991).
16. J. N. Abdurashitov, V. N. Gavrin, A. V. Kalikhov, *et al.*, Nucl. Instrum. Methods Phys. Res. A (Proc. Suppl.) **476**, 322 (2002).
17. J. N. Abdurashitov, E. L. Faizov, V. N. Gavrin, *et al.*, Phys. Lett. B **328**, 234 (1994).
18. S. R. Elliott, Nucl. Instrum. Methods Phys. Res. A **290**, 158 (1990).
19. B. T. Cleveland, Nucl. Instrum. Methods Phys. Res. A **214**, 451 (1983).
20. B. T. Cleveland, Nucl. Instrum. Methods Phys. Res. A **416**, 405 (1998).
21. V. N. Gavrin, Nucl. Phys. B (Proc. Suppl.) **91**, 36 (2001).
22. V. N. Gavrin, V. N. Kornoukhov, and V. É. Yants, Preprint IYaI AN SSSR P-0703 (1991).
23. V. N. Gavrin, S. N. Dan'shin, A. V. Kopylov, *et al.*, Preprint IYaI AN SSSR P-0494 (1986).
24. Ch. Evans Associated Report (unpublished).
25. V. N. Gavrin, V. V. Gorbachev, and I. N. Mirmov, Yad. Fiz. **65**, 1 (2002) [Phys. At. Nucl. **65**, 843 (2002)].
26. E. P. Veretenkin, V. N. Gavrin, A. M. Grigor'ev, *et al.*, At. Énerg. **72**, 260 (1992).
27. V. N. Gavrin and Yu. I. Zakharov, Preprint IYaI AN SSSR P-0560 (1987).
28. M. Cribier, B. Pichard, J. Rich, *et al.*, Astropart. Phys. **6**, 129 (1997).
29. V. N. Gavrin, V. V. Gorbachev, T. V. Ibragimova, and B. T. Cleveland, Yad. Fiz. **65**, 1309 (2002).
30. J. N. Abdurashitov, V. N. Gavrin, S. V. Girin, *et al.*, Phys. Rev. Lett. **77**, 4708 (1996).
31. J. N. Abdurashitov, V. N. Gavrin, S. V. Girin, *et al.*, hep-ph/9803418; Phys. Rev. C **59**, 2246 (1999).
32. W. Hampel and L. Remsberg, Phys. Rev. C **31**, 666 (1985).
33. V. Berezinsky, G. Fiorentini, and M. Lissia, hep-ph/9904225; Astropart. Phys. **12**, 299 (2000).
34. G. L. Fogli, E. Lisi, D. Montanino, *et al.*, hep-ph/9910387; Phys. Rev. D **61**, 073009 (2000).
35. J. Pulido and E. Kh. Akhmedov, hep-ph/9907399; Astropart. Phys. **13**, 227 (2000).
36. P. A. Sturrock and J. D. Scargle, astro-ph/0011228; Astrophys. J. **550**, L101 (2001).
37. J. N. Bahcall, M. H. Pinsonneault, and S. Basu, astro-ph/0010346; Astrophys. J. **555**, 990 (2001).
38. J. N. Bahcall, hep-ph/0108148; Phys. Rev. C **65**, 025801 (2002).
39. J. N. Bahcall, hep-ph/9710491; Phys. Rev. C **56**, 3391 (1997).
40. J. N. Bahcall, M. C. Gonzalez-Garcia, and C. Peña-Garay, hep-ph/0106258; JHEP **0108**, 014 (2001).
41. P. I. Krastev and A. Yu. Smirnov, hep-ph/0108177; Phys. Rev. D **65**, 073022 (2002).
42. M. C. Gonzales-Garcia, M. Maltoni, and C. Peña-Garay, hep-ph/0108073.

Translated by V. Astakhov